Published in final edited form as:
Mol Cell Neurosci. 2009 March ; 40(3): 390–400. doi:10.1016/j.mcn.2008.12.007.

N-cadherin modulates voltage activated calcium influx via RhoA, p120-catenin, and myosinactin interaction

Glen S. Marrs[1], **Christopher S. Theisen**, and **Juan L. Brusés**[*]
University of Kansas School of Medicine, Department of Anatomy and Cell Biology, Kansas City, KS 66160

Abstract

N-cadherin is a transmembrane adhesion receptor that contributes to neuronal development and synapse formation through homophilic interactions that provide structural-adhesive support to contacts between cell membranes. In addition, N-cadherin homotypic binding may initiate cell signaling that regulates neuronal physiology. In this study, we investigated signaling capabilities of N-cadherin that control voltage activated calcium influx. Using whole-cell voltage clamp recording of isolated inward calcium currents in freshly isolated chick ciliary ganglion neurons we show that the juxtamembrane region of N-cadherin cytoplasmic domain regulates high-threshold voltage activated calcium currents by interacting with p120-catenin and activating RhoA. This regulatory mechanism requires myosin interaction with actin. Furthermore, N-cadherin homophilic binding enhanced voltage activated calcium current amplitude in dissociated neurons that have already developed mature synaptic contacts *in vivo*. The increase in calcium current amplitude was not affected by brefeldin A suggesting that the effect is caused via direct channel modulation and not by increasing channel expression. In contrast, homotypic N-cadherin interaction failed to regulate calcium influx in freshly isolated immature neurons. However, RhoA inhibitors enhanced calcium current amplitude in these immature neurons, suggesting that the inhibitory effect of RhoA on calcium entry is regulated during neuronal development and synapse maturation. These results indicate that N-cadherin modulates voltage activated calcium entry by a mechanism that involves RhoA activity and its downstream effects on the cytoskeleton, and suggest that N-cadherin provides support for synaptic maturation and sustained synaptic activity by facilitating voltage activated calcium influx.

Keywords

N-cadherin; voltage activated calcium currents; RhoA GTPase; p120-catenin; cell adhesion; neural development; ciliary ganglion; cytoskeleton

[*] **Corresponding Author:** Juan L. Brusés, Kansas University Medical Center, Department of Anatomy and Cell Biology, 3901 Rainbow Blvd. MS 3038, Kansas City, KS 66160 Phone: 913-588-1790 Fax: 913-588-2710 jbruses@kumc.edu.
[1]Present Address: West Virginia University, Sensory Neuroscience Research Center, Morgantown, WV 26506

Introduction

The transmembrane adhesion receptor N-cadherin contributes to a variety of cellular and developmental processes by regulating cell-cell adhesion, cytoskeleton dynamics, and cell signaling (Gumbiner, 2005; Takeichi, 2007). In the nervous system, N-cadherin is expressed throughout development and becomes highly concentrated at synaptic junctions during the assembly of neuronal circuits (Uchida et al., 1996; Benson and Tanaka, 1998; Rubio et al., 2005). N-cadherin contributes to neural development and synapse formation by providing adhesive support between cell membranes (Brusés, 2000; Takeichi and Abe, 2005). In addition to its adhesive properties, N-cadherin homophilic binding regulates small Rho GTPases and the cytoskeleton (Fukata and Kaibuchi, 2001), which influence various aspect of cell physiology, suggesting that N-cadherin homotypic interaction may also regulate intracellular signaling mechanisms that contribute to the formation and function of the nervous system (Takeichi and Abe, 2005; Brusés, 2006; Arikkath and Reichardt, 2008).

N-cadherin belongs to the subfamily of classical type-1 cadherins (Hatta et al., 1988; Nollet et al., 2000). It is comprised of an extracellular domain with five cadherin repeats, a single pass transmembrane region, and a short cytoplasmic tail containing two main binding regions, the C-terminal domain and the juxtamembrane domain (JMD). The ectodomain homophilically binds in *cis* and in *trans* to establish adhesive bonds between cell membranes (Shapiro et al., 1995; Chitaev and Troyanovsky, 1998; Tamura et al., 1998; Troyanovsky et al., 2003; Troyanovsky et al., 2007). The C-terminal domain binds to β-catenin, which contributes to the recruitment of synaptic vesicles (Bamji et al., 2003). The JMD interacts with p120-catenin (Ohkubo and Ozawa, 1999; Anastasiadis and Reynolds, 2000), and regulates both cadherin adhesive activity and cytoskeletal dynamics (Yap et al., 1998; Aono et al., 1999; Anastasiadis et al., 2000; Ozawa, 2003). These two cadherin activities are highly interdependent, in that formation of adhesive bonds requires homophilic binding between cadherin ectodomains and cytoskeletal anchoring of cadherin intracellular domain, suggesting that cadherins activity is regulated in both directions across the cell membrane (Wheelock and Johnson, 2003; Gumbiner, 2005). The bi-directional signaling capabilities of cadherins are evidenced by the fact that protein interactions with the cadherin cytoplasmic tail affect the adhesive properties of the cell surface (inside-out) (Brieher and Gumbiner, 1994; Aono et al., 1999), while cadherin homophilic binding influences the actin cytoskeleton through the regulation of small Rho GTPases (outside-in) (Charrasse et al., 2002; Ehrlich et al., 2002; Lampugnani et al., 2002; Noren et al., 2003).

Small Rho GTPases and the cytoskeleton have been implicated in the regulation of voltage activated calcium channels (VACC) (Wilk-Blaszczak et al., 1997; Rueckschloss and Isenberg, 2001; Piccoli et al., 2004; Iftinca et al., 2007), suggesting that N-cadherin signaling regulates neuronal physiology by controlling intracellular Ca^{2+} levels. Voltage activated Ca^{2+} channels are abundantly expressed at presynaptic terminals and in certain postsynaptic structures (Stanley, 1991; White et al., 1997; Catterall, 2000). This type of ion channels are opened in response to neuronal depolarization and are essential for synaptic transmission by mediating Ca^{2+} influx required for synaptic vesicle fusion and neurotransmitter release (Wheeler et al., 1994; Fisher and Bourque, 2001). In addition, Ca^{2+} influx affects neuronal excitability and participates in long-term plastic changes by activating gene transcription (Takasu et al., 2002). The present study was designed to investigate whether N-cadherin signaling controls voltage activated Ca^{2+} influx. Using whole-cell voltage clamp recording of isolated inward Ca^{2+} currents in freshly dissociated chick ciliary ganglion neurons, this study examined the role of RhoA GTPase, the cytoskeleton, and N-cadherin homophilic binding in the regulation of voltage activated Ca^{2+} influx.

Results

To examine the mechanism by which N-cadherin regulates Ca^{2+} influx, high-threshold voltage activated (HVA) inward Ca^{2+} currents were recorded from the cell body of freshly dissociated chick ciliary ganglion neurons. Ciliary ganglion neurons abundantly express N-cadherin (Conroy et al., 2000; Rubio et al., 2005) and primarily express voltage activated Ca^{2+} channels (VACC) of the N-type (White et al., 1997). Figure 1A shows a group of representative traces of isolated HVA inward Ca^{2+} currents elicited by 100 msec duration voltage steps from a holding potential of −80 mV to a range of voltages (−50 to 50 mV). As was previously reported for ciliary ganglion neurons (White et al., 1997; Piccoli et al., 2004), inward Ca^{2+} currents are characterized by an initial peak that accelerates with the increase in voltage steps, which is followed by a slow inactivation of the current until the end of the pulse. Calcium currents were normalized to cell size using cell membrane capacitance and values expressed as current density (pA/pF). Experimental manipulations were accomplished by incorporating purified polypeptides into the intracellular solution loaded in the patch pipette for rapid infusion into cells upon patch rupture, by bath application of membrane permeable drugs, or by plating dissociated neurons on coverslips coated with recombinant protein. To evaluate the efficiency of protein delivery, recombinant EGFP (1 μM, 39kDa) was loaded into the patch pipette and cells were observed under fluorescence microscopy. Within 1-2 minutes after membrane patch rupture, EGFP fluorescence was detected throughout the cell body without affecting Ca^{2+} currents (data not shown; (Piccoli et al., 2004)). Measurements were obtained between 5-7 minutes after achieving whole-cell voltage-clamp configuration to ensure uniform access of delivered reagents and to minimize the effect of Ca^{2+} currents rundown.

N-cadherin JMD inhibits HVA inward Ca^{2+} currents by binding to p120-catenin and activating RhoA

To investigate whether protein interactions with N-cadherin cytoplasmic domain affect Ca^{2+} influx, we first examined the role of N-cadherin JMD on HVA inward Ca^{2+} currents. We focused on the N-cadherin JMD because this region of the cytoplasmic domain interacts with p120-catenin which regulates small Rho GTPase activity and cytoskeleton dynamics (Anastasiadis et al., 2000), and both of these mechanisms have been implicated in the regulation of voltage activated Ca^{2+} currents (Wilk-Blaszczak et al., 1997; Rueckschloss and Isenberg, 2001; Piccoli et al., 2004; Iftinca et al., 2007). The JMD is comprised of the N-terminus 87 amino acids of N-cadherin cytoplasmic domain and operates as a dominant-interfering polypeptide by interacting with proteins that bind to endogenous N-cadherin. Figure 1 shows the average current density-voltage plots for St 40 ciliary ganglion neurons and for neurons infused with recombinant chicken N-cadherin sJMD. Application of sJMD resulted in a substantial reduction of peak Ca^{2+} current amplitude as compared to control intracellular solution (Fig. 1B, *open triangles vs. circles*) (Piccoli et al., 2004).

To test whether binding of p120-catenin to sJMD is required for regulation of voltage activated Ca^{2+} influx, N-cadherin amino acids 780-782 were substituted for alanines (sJMD780AAA). Amino acids 780-782 are within the p120-catenin core binding region of N-cadherin cytoplasmic domain and their substitution for alanine blocks p120-catenin binding to the JMD (Anastasiadis et al., 2000; Thoreson et al., 2000). Infusion of sJMD-780AAA into St 40 ciliary ganglion neurons did not affect peak Ca^{2+} current amplitude, which is similar to control values (Fig. 1B, *squares vs. circles*). To confirm that mutated sJMD did not interact with p120-catenin, recombinant GST-tagged sJMD and sJMD780AAA were incubated with 6XHis-tagged p120-catenin (p120-228) (Fig. 1C). The first 227 amino acids were removed to facilitate protein production (see methods). Deletion of these amino acids does not interfere with the ability of p120-catnein to bind cadherin JMD (Aono et al., 1999). The protein complexes were pull-down with glutathione-conjugated agarose beads, and analyzed by Western blot using anti-His

antibodies (Fig 1C). A substantial amount of p120-catenin was recovered form the samples incubated with sJMD (lane 4) while a very small amounts of p120-catenin were detected from the samples incubated with sJMD-780AAA (lane 3), indicating that triple alanine substitution of amino acid residues 780-782 disrupted p120-catenin/sJMD interaction. Thus, the inability of sJMD-780AAA to modulate Ca^{2+} currents together with its failure to associate with p120-catenin indicates that binding to p120-catenin is necessary for sJMD mediated regulation of HVA Ca^{2+} current amplitude.

The effect of the sJMD on HVA Ca^{2+} current amplitude is attributed to the activation of RhoA because simultaneous application of sJMD with the RhoA inhibitor C3 exotransferase largely alleviates the suppressive effect of sJMD (Fig. 1B, *open diamonds*) (Piccoli et al., 2004). To further test the involvement of RhoA in regulation of VACC, a constitutively active form of RhoA (Q63L, 0.4μM) was infused into St 40 ciliary ganglion neurons during voltage-clamp recording of HVA Ca^{2+} currents. This dominant-active form of RhoA (DA-RhoA) caused a substantial decrease in averaged peak Ca^{2+} current comparable to the effect of the sJMD (Fig. 1D, *open squares*), indicating that active RhoA inhibits voltage activated Ca^{2+} influx. Moreover, analysis of the voltage dependence of current activation (Pattillo et al., 1999) showed that sJMD and DA-RhoA did not affect the voltage dependence of the current gating (Fig 1E). Simultaneous application of both DA-RhoA and sJMD did not result in further inhibition of averaged peak Ca^{2+} current amplitude (Fig. 1D, *diamonds*), suggesting that sJMD signaling and RhoA activation share a common pathway for modulation of VACC and that both treatments operate through a similar mechanism.

Inhibition of myosin-actin interaction blocks the effect of sJMD on HVA inward Ca^{2+} currents

RhoA activates a variety of down-stream effectors which regulate the cytoskeleton (Bishop and Hall, 2000). Thus, to determine whether changes in cytoskeletal dynamics mediate the effect of sJMD on VACC activity, the role of myosin was examined by observing the effect of the myosin inhibitor blebbistatin on Ca^{2+} current regulation. Blebbistatin is a membrane permeable small molecule that binds to myosin and blocks myosin-actin interaction, without affecting light chain kinase activity and myosin phosphorylation (Cheung et al., 2002; Straight et al., 2003). Bath application of blebbistatin (50 μM) did not affect Ca^{2+} current amplitude in St 40 ciliary ganglion neurons (Fig. 2A, *triangles*). However, blebbistatin completely reverted the inhibitory effect of sJMD on Ca^{2+} current amplitude (Fig. 2A, *open circles*). Photo-inactivated blebbistatin was no longer capable of blocking sJMD mediated Ca^{2+} current inhibition (Fig. 2A, *diamonds*), indicating that sJMD regulation of HVA inward Ca^{2+} currents requires myosin interaction with actin. Furthermore, to examine whether activation of actin-myosin interaction affects Ca^{2+} influx, we tested the effect of intracellular application of a peptide that constitutively activates myosin light chain kinase (MLCK) (Polo-Parada et al., 2005). MLCK phosphorylates myosin and promotes its binding to actin. Infusion of MLCK agonist (1 μM) decreased average peak Ca^{2+} current amplitude to a similar extent as sJMD and DA-RhoA did (Fig. 2B, *open squares*), suggesting that myosin interaction with actin participates in the regulation of channel activity. These results indicate that activation of RhoA by sJMD is capable of affecting VACC activity and that this mechanism involves p120-catenin and actin-myosin interaction.

N-cadherin homophilic binding enhances HVA Ca^{2+} influx

In the previous sections of this study we described an intracellular pathway by which the interaction between N-cadherin JMD and p120-catenin activates RhoA and inhibits HVA Ca^{2+} influx via a mechanism that requires myosin activity. To examine whether N-cadherin homophilic binding was sufficient to modulate voltage activated Ca^{2+} influx, HVA inward Ca^{2+} current densities were measured in freshly dissociated St 40 ciliary ganglion neurons plated on coverslips coated with recombinant chicken N-cadherin ectodomain C-terminally

fused to an immunoglobulin G (IgG) Fc fragment (Fc-N-cadherin). Figure 3A depicts the average density currents of St 40 ciliary neurons plated on Fc-N-cadherin substrate. The averaged peak Ca^{2+} current was enhanced by 36% within 1-3 hours of presentation to Fc-N-cadherin, as compared to neurons plated on a Con A substrate (Fig. 3A, *open diamonds vs. circles*), without affecting the voltage dependence of the current gating (Fig 3D). Neurons plated on a BSA substrate showed Ca^{2+} current amplitudes similar to the neurons plated on Con A (35.2 ± 2.3 pA/pF, n= 11). Furthermore, to examine whether the increase of HVA Ca^{2+} influx caused by the N-cadherin homophilic binding was specific for N-cadherin or was due to an overall increase in cell adhesion, neurons were plated on a laminin substrate for the same amount of time. In contrast to Fc-N-cadherin, no changes in HVA inward Ca^{2+} current amplitude were observed on cells plated on coverslips coated with laminin (Fig 3A, *open squares*).

To determine whether homophilic binding with full length N-cadherin expressed on the cell surface is also capable of regulating voltage activated Ca^{2+} influx, dissociated ciliary neurons were plated on top of Chinese Hamster Ovary (CHO) cells expressing full length chicken N-cadherin C-terminally fused to EGFP (Fig 3B, *triangles*). Co-culturing dissociated neurons with CHO cells expressing N-cadherin resulted in a 22% enhancement of Ca^{2+} current amplitude as compared to neurons plated on parental CHO cells (Fig 3B *circles*), which do not express N-cadherin (Fig 3E). Thus, these experiments indicate that N-cadherin homophilic interaction is sufficient to activate a cellular mechanism that regulates voltage-activated Ca^{2+} influx.

The enhancement HVA Ca^{2+} influx induced by N-cadherin homophilic binding was evaluated after 1-3 h of cell-substrate interaction. Therefore, it is possible that the increase in current amplitude was caused by insertion of new channels in the cell membrane and not by direct regulation of channel activity. To examine whether the increase in HVA inward Ca^{2+} current amplitude was due to insertion of additional VACC into the plasma membrane, dissociated St 40 ciliary ganglion neurons plated on Fc-N-cadherin substrate were treated for 2 hours with the protein transport inhibitor brefeldin A (Doms et al., 1989) (5 μg/mL) before assessing voltage activated Ca^{2+} influx. Treatment with brefeldin A did not interfere with the enhancement in Ca^{2+} current amplitude caused by N-cadherin homophilic binding (Fig. 3C, *open triangles*), indicating that averaged peak Ca^{2+} current enhancement promoted by N-cadherin engagement is unlikely to be caused by an increase in the concentration of channels at the cell membrane, but rather by a direct modulation of the channels. Finally, to determine whether N-cadherin-mediated regulation of HVA Ca^{2+} influx involves actin-myosin interactions, we examined the effect of blebbistatin on the HVA Ca^{2+} influx on neurons plated on N-cadherin substrate. Treatment with blebbistatin blocked the enhancement of HVA Ca^{2+} influx caused by N-cadherin homophilic binding (Fig 3C, *open squares*), indicating that changes in cytoskeletal dynamics downstream of N-cadherin engagement are necessary for the regulation of channel function.

Formation and maturation of synaptic contact in the chick ciliary ganglion are associated with changes in the distribution and composition of the N-cadherin complex (Rubio et al., 2005). At immature ciliary neurons (St 34-35), N-cadherin is distributed over the surface of the neurons with a mix of diffused and clustered patterns which are associated with p120-catenin. In contrast, mature neurons (St 40) have well-defined N-cadherin clusters on the cell surface, which are 70% larger than the ones formed on St 34-35 ciliary neurons, and appear to be less associated with p120-catenin (Rubio et al., 2005). The developmental changes in N-cadherin distribution in the ciliary ganglion suggest that N-cadherin engagement increases with neuronal maturation. In addition, HVA Ca^{2+} current amplitudes increase with neuronal maturation (White et al., 1997) (Fig 4B). Therefore, we examined whether the reduced levels in HVA Ca^{2+} current density observed in St 35 neurons could also be ameliorated by N-cadherin

homophilic binding. Freshly dissociated St 35 ciliary ganglion neurons were plated on Con A or on Fc-N-cadherin substrate for 1-3 h and their HVA Ca^{2+} current densities were analyzed (Fig 4A). In contrast to the enhancement of HVA Ca^{2+} influx observed in mature (St 40) neurons (Fig 3A), N-cadherin homophilic binding did not significantly affect inward Ca^{2+} currents on younger (St 35) neurons (St 35) (Fig 4A, *squares*), although and slight increase in Ca^{2+} current amplitude was observed. This result indicates that N-cadherin expressed on the surface of immature neurons is incapable of efficiently transducing signals into the cell that regulate HVA Ca^{2+} influx.

RhoA mediated inhibition of HVA inward Ca^{2+} current is developmentally regulated

Cadherin homophilic binding induces cadherin clustering, increases cell-cell adhesion, and regulates RhoA activity (Yap et al., 1997; Noren et al., 2001; Noren et al., 2003). Therefore, the increase in N-cadherin cluster size associate with synaptic maturation suggests that N-cadherin adhesion and signaling progressively increase with neuronal and synapse development. Thus, to investigate whether maturation of ciliary ganglion neurons is paralleled by changes in the level of RhoA activity we looked at the distribution of ezrin in St 35 and St 40 intact ciliary ganglia. The localization of ezrin at the cell membrane is downstream of RhoA signaling, and its distribution was used here as a marker of RhoA activity (Anastasiadis et al., 2000). Figure 5 shows St 35 and St 40 ciliary ganglion neurons immunostained with anti-ezrin and anti-N-cadherin (NCD2) antibodies. While ezrin localizes to the cell membrane in St 35 neurons, it is largely translocated to the cytoplasm at St 40, suggesting that St 35 ciliary neurons have higher endogenous levels of RhoA activity, which decrease with neuronal maturation and N-cadherin clustering. We also examined the overall cellular levels of active RhoA in the ciliary ganglion by using pull-down assays to assess the amount of RhoA binding to its effector rhotekin; however, this assay yielded no detectable differences between the two developmental stages (data not shown). In addition to examining the distribution of ezrin, we looked at F-actin localization in young and matured neurons by labeling actin filaments with phalloidin (Vandekerckhove et al., 1985). F-actin is diffusely distributed throughout the cytoplasm in St 35 neurons, while it forms a thick cortical cytoskeleton in St 40 neurons, indicating that synaptic maturation and N-cadherin clustering is associated with the re-organization of the actin cytoskeleton (Fig 5 g and h), as has been observed in cultured hippocampal neurons (Zhang and Benson, 2001).

To determine whether higher levels of endogenous RhoA activity affect Ca^{2+} currents, we assessed the effect of RhoA inhibitors on HVA inward Ca^{2+} current density in St 35 and St 40 ciliary ganglion neurons. Averaged peak Ca^{2+} currents densities in St 35 neurons were lower as compared to St 40 neurons (Fig 6A *open circles*) (White et al., 1997). However, application of the RhoA inhibitor C3 exotransferase into St 35 neurons resulted in a substantial enhancement of peak Ca^{2+} current density (Fig 6A *open diamonds*). In contrast, application of C3 exotransferase into St 40 neurons did not have a significant impact on Ca^{2+} current amplitude as compared to control cells (Fig 6B, *diamonds vs circles*). These results indicate that higher levels of endogenous RhoA activity appear to inhibit inward Ca^{2+} currents in younger neurons but that this mechanism is no longer active after neurons have matured.

Membrane localization of p120-catenin depends on its binding to cadherin JMD. Loss of cadherin expression or expression of mutated cadherins incapable of binding to p120-catenin result in the translocation of p120-catenin form the cell membrane to the cytosolic (Anastasiadis et al., 2000; Rubio et al., 2005). Furthermore, the increase in cytosolic concentration of p120-catenin inhibits RhoA activity (Anastasiadis et al., 2000). Therefore, we examined whether increasing cytosolic p120-catenin affects Ca^{2+} current amplitude. Indeed, infusion of recombinant p120-catenin into St 35 ciliary ganglion neurons resulted in a significant increase in Ca^{2+} current amplitude as compared to controls (Fig 6A *open triangles*

vs open circles). The magnitude of the increase was similar to the one obtained by inhibiting RhoA activity with C3 exotransferase. In contrast, infusion of p120-catenin into St 40 ciliary neurons had no significant effect on peak Ca^{2+} current amplitude (Fig 6B, *triangles*), as was observed with application of C3 exotransferase. These results further indicate that HVA Ca^{2+} influx in ciliary ganglion neurons is regulated by RhoA activity.

Discussion

Several lines of evidence indicate that N-cadherin homophilic binding contributes to synapse formation and synaptic transmission (Takeichi and Abe, 2005; Brusés, 2006; Arikkath and Reichardt, 2008). N-cadherin localizes at synaptic contacts from the onset of synaptogenesis, and synapse maturation is accompanied by the clustering of N-cadherin at synaptic sites (Yamagata et al., 1995; Fannon and Colman, 1996; Uchida et al., 1996; Benson and Tanaka, 1998; Rubio et al., 2005). N-cadherin clustering is also induced by synaptic activity and correlates with synaptic potentiation (Bozdagi et al., 2000). Moreover, blocking N-cadherin homophilic interaction affects the accumulation of synaptic proteins, synaptic vesicle recycling (Togashi et al., 2002; Bozdagi et al., 2004), and potentiation of neurotransmission (Bozdagi et al., 2000; Tanaka et al., 2000; Jungling et al., 2006), indicating that N-cadherin homotypic binding plays an important role in the assembly of synaptic connections and in the modulation of synaptic transmission by providing structural support to the synaptic complex and/or by activating intracellular signaling that regulates neuronal physiology.

In this study we used freshly dissociated primary neurons to characterize a mechanism by which N-cadherin modulates HVA Ca^{2+} influx. We used two main types of experimental manipulations to reveal certain components of this pathway. On the one hand, binding of endogenous N-cadherin with recombinant N-cadherin ectodomain was used to assess whether N-cadherin homophilic binding controls Ca^{2+} channel activity. On the other hand, infusion of recombinant N-cadherin JMD alone or in combination with pharmacological agents was used to determine whether certain protein interactions with N-cadherin cytoplasmic tail are capable of modulating downstream effectors that affect Ca^{2+} influx. Finally, as the distribution and composition of the N-cadherin complex changes during development of the ciliary neurons (Rubio et al., 2005), and these changes correlate with synaptic maturation and enhancement of Ca^{2+} influx (White et al., 1997; Brusés et al., 2002), we analyzed neurons from different developmental stages to infer whether changes in N-cadherin can be associated with its ability to regulate neuronal physiology.

Infusion of recombinant N-cadherin JMD into ciliary neurons causes a substantial reduction in peak Ca^{2+} current amplitude. This effect is mediated by the binding of JMD to p120-catenin and the activation of RhoA, indicating that RhoA negatively affects Ca^{2+} influx and that the level of RhoA activity in primary neurons can be manipulated by the interaction of p120-catenin with N-cadherin JMD (Fig 7). These results are in agreement with a previous report indicating that p120-catenin inhibits RhoA and this activity is affected by p120-catenin interaction with the JMD (Anastasiadis et al., 2000). However, recent evidence also indicates that p120-catenin is required to be localized close to the cell membrane and interacting with N-cadherin to locally and transiently inhibit RhoA by binding to p190RhoGAP (Wildenberg et al., 2006). Therefore, infusion of N-cadherin JMD can disrupt the interaction of p120-catenin that is localized to the cell membrane and associated with N-cadherin, or disrupt a cytosolic pool of p120-catenin that inhibits RhoA activation. Our experiments do not discriminate between these two possibilities. However, we can conclude that acute sequestration of a pool of p120-catenin by N-cadherin JMD results in the activation of RhoA which affects Ca^{2+} channel activity. Therefore, we infer from these experiments that physiological regulation of N-cadherin/p120-catenin interactions modulate RhoA activity and HVA Ca^{2+} influx.

We observed that N-cadherin homophilic binding enhances HVA Ca^{2+} influx in dissociated mature (St 40) ciliary ganglion neurons. In contrast, N-cadherin homophilic binding did not significantly enhance Ca^{2+} currents in immature (St 35) neurons, indicating that N-cadherin expressed on the surface of younger neurons was incapable of activating a cellular mechanism that regulates HVA Ca^{2+} influx. In a previous study we showed that at St 35, N-cadherin is dispersed on the surface of ciliary ganglion neurons and it is associated with p120-catenin (Rubio et al., 2005). These neurons possess immature synaptic contacts, poorly developed synaptic junctions, and have smaller Ca^{2+} current amplitudes as compared to mature neurons (White et al., 1997; Brusés et al., 2002). St 40 neurons have formed mature synaptic contacts and larger N-cadherin clusters in the proximity of the active zone, which are less associated with p120-catenin (Rubio et al., 2005). Therefore, the changes in the distribution and composition of the N-cadherin complex appear to be associated with its ability to regulate Ca^{2+} influx. As p120-catenin inhibits RhoA activity, and this inhibition is affected by the binding of p120-catenin to cadherin JMD (Anastasiadis et al., 2000), the uncoupling of p120-catenin associated with neuronal maturation may indicate that changes in the localization of p120-catenin are associated with its ability to regulate RhoA and Ca^{2+} influx. This view is supported by the fact that acute application of RhoA inhibitors (C3 exotransferase and p120-catenin) to mature (St 40) neurons has little effect on channel activity, suggesting that at this stage there are low levels of endogenous RhoA activity that regulates Ca^{2+} influx. In contrast, infusion of RhoA inhibitors into immature (St 35) neurons results in a significant increase in peak Ca^{2+} current amplitude, indicating that younger neurons possess a higher level of endogenous RhoA activity. Interestingly, N-cadherin engagement did not affect Ca^{2+} influx in younger (St 35) neurons, suggesting that the composition of the N-cadherin complex at this stage does not regulate the activity of RhoA that is involved in the modulation of channel function. Although regulation of RhoA activity has been reported to be downstream of cadherin engagement (Noren et al., 2001; Noren et al., 2003), we can not conclude from our experiments whether regulation of RhoA is downstream of N-cadherin homophilic binding in primary neurons which affects directly or indirectly Ca^{2+} channel activity. Regulation of channel function via N-cadherin homophilic binding may be more complex than the inhibition of RhoA activity, in that activation of RhoA has different effects depending on the downstream effectors. For instance, RhoA activation enhances adherens junction formation by activating mDia1, while activation of ROCK may induce cadherin mediated junctions disassembly (Sahai and Marshall, 2002; Carramusa et al., 2007). Therefore, activation of different RhoA effectors may be involved in the assembly of the N-cadherin signaling complex and in the regulation of channel activity (Shewan et al., 2005; Miyake et al., 2006). Regulation of different RhoA effectors may also explain why inhibition and enhancement of HVA Ca^{2+} influx are both equally affected by the blockade of myosin interaction with actin.

We focused our attention on VACC because these channels are important for regulation of intracellular Ca^{2+}, which plays a central role in neurotransmitter release and neuronal excitability. VACC in primary neurons are regulated by a variety of mechanisms (Catterall, 2000) including small Rho GTPases (Piccoli et al., 2004; Iftinca et al., 2007), and changes in the state of actin polymerization and actin-myosin interaction (Fukuda et al., 1981; Johnson and Byerly, 1993; Rueckschloss and Isenberg, 2001). These studies support a model whereby allosteric interactions between the actin cytoskeleton and VACC regulate channel function (Johnson and Byerly, 1993). However, the molecular mechanisms that reside up-stream of the cytoskeleton, which could regulate gating properties of Ca^{2+} channels have not been extensively characterized. Here, we provide evidence that regulation of RhoA by N-cadherin JMD and p120-catenin affects HVA Ca^{2+} influx by a mechanism that involves actin-myosin interaction, suggesting that channel function can be regulated by extracellular signals that control RhoA activity and cytoskeletal dynamics. Although the RhoA effector ROCK inhibits Ca^{2+} influx by phosphorylating the channel a-subunit (Iftinca et al., 2007), we observed that the inhibitory effect of RhoA on channel function requires myosin-actin interaction. This

suggests that channel modifications caused by phosphorylation need an active cytoskeleton to influence channel activity, or that different RhoA effectors may control channel responsiveness through distinct mechanisms.

Ciliary neurons are the postsynaptic element of the calyciform synapses formed in the ciliary ganglion. HVA Ca^{2+} currents in these neurons are almost entirely driven by HVA N-type Ca^{2+} channels (White et al., 1997; Piccoli et al., 2004). N-type Ca^{2+} channels are highly expressed at presynaptic terminals and mediate the influx of Ca^{2+} required for synaptic vesicle fusion and neurotransmitter release (Wheeler et al., 1994; Fisher and Bourque, 2001). Therefore, the N-cadherin mediated modulation of channel function that we described in postsynaptic ciliary neuron bodies could be generalized to N-type channels located at presynaptic terminals. If this is the case, formation of N-cadherin mediated adherens junctions at synaptic contacts will enhance Ca^{2+} influx at the active zones. As the relationship between Ca^{2+} influx and transmitter release is exponential (Augustine and Charlton, 1986), small changes in Ca^{2+} influx have a substantial impact in neurotransmitter release. Thus, the increase in voltage activated Ca^{2+} influx caused by N-cadherin homophilic binding in ciliary neurons may significantly enhance the amount of transmitter release and the efficacy of synaptic transmission.

Previous analyses have indicated that synaptic transmission at synaptic contacts formed between N-cadherin null neurons show defects in short-term plasticity induced by repetitive stimulation (Jungling et al., 2006). These deficits appear to be caused by a reduction in the availability of synaptic vesicles in the readily-releasable pool (Bamji et al., 2003; Jungling et al., 2006). However, removal of N-cadherin at presynaptic terminals reduces synaptic response to single action potentials, suggesting that N-cadherin homophilic binding between synaptic compartments regulate neurotransmitter release (Jungling et al., 2006). Therefore, regulation of HVA Ca^{2+} currents by N-cadherin homophilic binding may explain the deficits in synaptic physiology observed when N-cadherin expression or function has been impaired.

In summary, our study shows that N-cadherin homophilic binding is capable of enhancing HVA Ca^{2+} currents in primary neurons, and provide evidence for a functional role of N-cadherin acting as a contact-dependant signaling receptor on neuronal physiology. As both, neurotransmitter release and postsynaptic responses are regulated by Ca^{2+} influx, N-cadherin-mediated signaling within the synaptic junctional complex may result in an enhancement of synaptic efficacy through the increase in intracellular Ca^{2+} concentrations. This mechanism may explain the role of N-cadherin in long and short-term plastic changes in synaptic transmission (Bozdagi et al., 2000; Jungling et al., 2006). Therefore, the molecular mechanisms that regulate the assembly of the N-cadherin signaling complex should have important implications for synapse development and for the physiology of synaptic transmission.

Experimental methods

Animals

Fertilized White Leghorn chicken eggs obtained from a local farm were incubated in a forced-draft incubator at 39°C under a humidified atmosphere until the desired developmental stage (St) (Hamburger and Hamilton, 1951) was reached.

cDNA Constructs

N-cadherin-EGFP: Full-length chicken N-cadherin cDNA (a gift from Dr. M. Takeichi, RIKEN Center, Kobe, Japan) was C-terminally fused to EGFP in pEGFP-N1 (Clontech, Mountain View, CA). N-cadherin soluble JMD (sJMD): The JMD of chicken N-cadherin (from Lys 753 to Gly 839) was PCR amplified and cloned into pQE-60 vector (Qiagen, Chatsworth,

CA) to fuse a 6X histidine (His) tag at the C-terminus. N-cadherin JMD-780AAA: Amino acid residues 780-782 were substituted for alanines using the QuikChange site-directed mutagenesis kit (Stratagene, La Jolla, CA). The mutated sequence was PCR amplified and His tagged using pQE60. JMD-glutathione-Stransferase (GST) and JMD-780AAA-GST: To N-terminally fuse a GST tag to JMD and JMD-AAA, PCR strategies were used to insert JMD fragments in the GST-tagging vector pGEX4T-3 (GE Healthcare, Piscataway, NJ). p120-228: pRC/CMV-p120 (a gift from Dr. A. Reynolds, Vanderbilt University, Nashville, TN) was used as template to PCR amplify mouse N-terminally truncated p120-catenin. The first 227 amino acids were removed to facilitate protein production. An ATG start site and a NcoI restriction site were created at position 685. p120-228 cDNA was ligated in pET16b (Novagen, Madison, WI) to N-terminally 6X His tag the protein. All sequences were examined by sequencing analysis.

Synthesis and Isolation of Recombinant Proteins

Polypeptides were generated and purified using standard chromatography techniques. Briefly, plasmids were transfected into M15 or BL21 cells, and protein expression was induced by IPTG (1 mM). The cells were grown for 4 hr at 37°C, lysed, recombinant protein purified on a nickel or glutathione column, examined by SDS-PAGE, and dialyzed against intracellular solution. Protein concentration was determined by BCA assay (Pierce, Rockford, IL). Chicken N-cadherin ectodomain fused to mouse IgG Fc domain (a gift from Dr. R.M. Mege, INSERM, U706, Universite Pierre et Marie Curie, 75005 Paris, France) was transfected into Human Embryonic Kidney (HEK) 293 cells using Liptofectamine 2000 (Invitrogen, Carlsbad, CA). Secreted N-cadherin-Fc was collected in serum-free culture media and concentrated using a Centricon Ultracel YM-100 (Millipore, Billerica, MA). Constitutively active form of human RhoA (Q63L) was obtained from Cytoskeleton Inc. (Denver, CO).

In Vitro Binding Assays

Purified JMD-GST or JMD-780AAA-GST (50 μg) was immobilized on 25 μl glutathione-agarose resin (Sigma, G4510) and incubated with 100 μg purified, His-tagged p120-228. The samples were washed 5 times with Tris buffer saline (10 mM Tris-HCl, pH 8.0, 9 g/l NaCl) with 0.05% Tween 20. Samples were then resolved by SDS-PAGE and transferred to a nitrocellulose membrane. A Western blot was performed to detect the presence of p120-228 using mouse anti-poly-His tag antibody (Sigma, H1029) and a goat peroxidase-conjugated anti-mouse secondary antibody (Jackson Immuno Research Laboratories, West Grove, PA).

Cell Dissociation and Culture

Ciliary ganglia were dissected in 12°C Tyrode's solution and collected in extracellular solution (in mM) 130 NaCl, 5 KCl, 1 $MgCl_2$, 1.2 $CaCl_2$, 10 Hepes, 11 glucose, pH 7.4. Tissue was incubated (23 min at 37°C) with type IV collagenase (0.45 mg/mL; Worthington Biochemical, Lakewood, NJ), hyaluronidase (10,000 U/mL; EMD Biosciences, San Diego, CA), and trypsin inhibitor (15 ng/mL; Sigma, St. Louis, MO), rinsed at 12°C in extracellular solution containing 10% FBS to inhibit enzymes, dissociated with a fire-polished Pasteur pipette in 37°C DME plus 21 mM $NaHCO_3$, transferred to concanavalin A (Con A) treated (250 ng/mL) plastic coverslip, and kept in a 37°C tissue culture incubator with 5% CO_2 (50 min-2h) before initiating patch clamp recording. CHO cells stably transfected with N-cadherin-EGFP were maintained in DME containing 10% FBS, and grown to 80% confluence. CHO cells were washed prior to the addition of dissociated ciliary neurons. Co-cultures were maintained in a tissue incubator for 2-8 hr in serum-free DME. A stable N-cadherin CHO cell line was generated by clonal isolation of cells expressing full-length N-cadherin EGFP fusion protein and a neomycin resistance gene and maintained with geneticin (0.5mg/mL).

Whole Cell Voltage Clamp Recording

Ca^{2+} currents were recorded at a −80 mV holding potential in whole-cell patch clamp configuration, using a Multiclamp 700A amplifier (Axon Instruments, USA), connected to a Digidata 1322A analogue-to-digital converter. Borosilicate glass capillaries (type 8250, 1.5 mm O.D., 1.1 mm I.D.; Garner Glass, Claremont, CA) were pulled using a two-stage vertical puller (David Kopf 730), and heat-polished to yield a resistance of 2-5 MΩ. Intracellular solution utilized contained (in mM): CsCl 140, NaOH 10, $MgCl_2$ 1, BAPTA 0.5, Hepes 20, ATP-Mg 5, GTP-Na 0.2, mannitol 4.7, pH 7.4. Series resistance was compensated 50-80% before each recording. For Ca^{2+} current isolation, extracellular solution contained (in mM): 140 Tetraethylammonium chloride, 5 $CaCl_2$, 1 $MgCl_2$, 10 Hepes, 11 glucose, pH 7.4, and 3 μM tetrodotoxin. Currents were elicited and acquired using pClamp9 software. Voltage dependence and kinetics of ciliary neurons Ca^{2+} currents were determined as previously described (Pattillo et al., 1999) by using 10 ms voltage steps from −50 mV to 50 mV. After stepping back to −80 mV the peak of the tail current was used as an estimate of the steady-state activation of Ca^{2+} currents and those data were fitted with a Boltzmann function. Raw data were analyzed and plotted using Clampfit 9.0 software. Ca^{2+} current amplitudes were normalized to membrane capacitance (pA/pF). Values are expressed as the mean of each group ± SE. Statistical significance was assessed by the Student's *t* test.

Immunocytochemistry

Ciliary ganglia were fixed in 2% paraformaldehyde in 0.1M phosphate buffer, pH7.2 and 15% water saturated picric acid for 20 min at room temperature and immunostained as previously described (Rubio et al., 2005). Actin filaments (F-actin) were detected with Alexa Fluor 488-phalloidin (Molecular Probes, Eugene, OR). Confocal microscopy: LSM510 Zeiss confocal microscope mounted on an Axioplan II Zeiss microscope (Zeiss, Oberkochen, Germany) with a C-Apochromat 63X/1.2 Zeiss water immersion lens. Nikon C1-SI confocal microscope mounted on a Nikon Eclipse 90i up-right microscope with a Plan Apo 60X/1.4 Nikon oil immersion lens. Optical sections were collected at 1 μm intervals independently from each fluorochrome using the manufacturers software. Primary antibodies: NCD2, rat monoclonal against chicken N-cadherin (Hatta et al., 1988), Zymed 13-2100 (South San Francisco, CA); mouse monoclonal against murine p120-catenin (Wu et al., 1998), Zymed 33-9700; mouse monoclonal against human ezrin BD Transduction Laboratories 610602 (San Jose CA).

Acknowledgments

This work was supported by a National Institutes of Health Grant NS40300 awarded to J.L. Brusés and by a Lied Endowed Grant from the Kansas University Research Institute. We thank Dr. Steve D. Meriney for his critical reading and useful comments on the manuscript.

References

Anastasiadis PZ, Reynolds AB. The p120 catenin family: complex roles in adhesion, signaling and cancer. J Cell Sci 2000;113(Pt 8):1319–1334. [PubMed: 10725216]

Anastasiadis PZ, Moon SY, Thoreson MA, Mariner DJ, Crawford HC, Zheng Y, Reynolds AB. Inhibition of RhoA by p120 catenin. Nat Cell Biol 2000;2:637–644. [PubMed: 10980705]

Aono S, Nakagawa S, Reynolds AB, Takeichi M. p120(ctn) acts as an inhibitory regulator of cadherin function in colon carcinoma cells. J Cell Biol 1999;145:551–562. [PubMed: 10225956]

Arikkath J, Reichardt LF. Cadherins and catenins at synapses: roles in synaptogenesis and synaptic plasticity. Trends Neurosci. 2008

Augustine GJ, Charlton MP. Calcium dependence of presynaptic calcium current and post-synaptic response at the squid giant synapse. J Physiol 1986;381:619–640. [PubMed: 2442355]

Bamji SX, Shimazu K, Kimes N, Huelsken J, Birchmeier W, Lu B, Reichardt LF. Role of beta-catenin in synaptic vesicle localization and presynaptic assembly. Neuron 2003;40:719–731. [PubMed: 14622577]

Benson DL, Tanaka H. N-cadherin redistribution during synaptogenesis in hippocampal neurons. J Neurosci 1998;18:6892–6904. [PubMed: 9712659]

Bishop AL, Hall A. Rho GTPases and their effector proteins. Biochem J 2000;348(Pt 2):241–255. [PubMed: 10816416]

Bozdagi O, Shan W, Tanaka H, Benson DL, Huntley GW. Increasing numbers of synaptic puncta during late-phase LTP: N-cadherin is synthesized, recruited to synaptic sites, and required for potentiation. Neuron 2000;28:245–259. [PubMed: 11086998]

Bozdagi O, Valcin M, Poskanzer K, Tanaka H, Benson DL. Temporally distinct demands for classic cadherins in synapse formation and maturation. Mol Cell Neurosci 2004;27:509–521. [PubMed: 15555928]

Brieher WM, Gumbiner BM. Regulation of C-cadherin function during activin induced morphogenesis of Xenopus animal caps. J Cell Biol 1994;126:519–527. [PubMed: 8034750]

Brusés JL. Cadherin-mediated adhesion at the interneuronal synapse. Curr Opin Cell Biol 2000;12:593–597. [PubMed: 10978895]

Brusés JL. N-cadherin signaling in synapse formation and neuronal physiology. Molecular Neurobiology 2006;33:237–252. [PubMed: 16954598]

Brusés JL, Chauvet N, Rubio ME, Rutishauser U. Polysialic acid and the formation of oculomotor synapses on chick ciliary neurons. J Comp Neurol 2002;446:244–256. [PubMed: 11932940]

Carramusa L, Ballestrem C, Zilberman Y, Bershadsky AD. Mammalian diaphanous-related formin Dia1 controls the organization of E-cadherin-mediated cell-cell junctions. J Cell Sci 2007;120:3870–3882. [PubMed: 17940061]

Catterall WA. Structure and regulation of voltage-gated Ca2+ channels. Annu Rev Cell Dev Biol 2000;16:521–555. [PubMed: 11031246]

Charrasse S, Meriane M, Comunale F, Blangy A, Gauthier-Rouviere C. N-cadherin-dependent cell-cell contact regulates Rho GTPases and beta-catenin localization in mouse C2C12 myoblasts. J Cell Biol 2002;158:953–965. [PubMed: 12213839]

Cheung A, Dantzig JA, Hollingworth S, Baylor SM, Goldman YE, Mitchison TJ, Straight AF. A small-molecule inhibitor of skeletal muscle myosin II. Nat Cell Biol 2002;4:83–88. [PubMed: 11744924]

Chitaev NA, Troyanovsky SM. Adhesive but not lateral E-cadherin complexes require calcium and catenins for their formation. J Cell Biol 1998;142:837–846. [PubMed: 9700170]

Conroy WG, Ogden LF, Berg DK. Cluster formation of alpha7-containing nicotinic receptors at interneuronal interfaces in cell culture. Neuropharmacology 2000;39:2699–2705. [PubMed: 11044740]

Doms RW, Russ G, Yewdell JW. Brefeldin A redistributes resident and itinerant Golgi proteins to the endoplasmic reticulum. J Cell Biol 1989;109:61–72. [PubMed: 2745557]

Ehrlich JS, Hansen MD, Nelson WJ. Spatio-temporal regulation of Rac1 localization and lamellipodia dynamics during epithelial cell-cell adhesion. Dev Cell 2002;3:259–270. [PubMed: 12194856]

Fannon AM, Colman DR. A model for central synaptic junctional complex formation based on the differential adhesive specificities of the cadherins. Neuron 1996;17:423–434. [PubMed: 8816706]

Fisher TE, Bourque CW. The function of Ca(2+) channel subtypes in exocytotic secretion: new perspectives from synaptic and non-synaptic release. Prog Biophys Mol Biol 2001;77:269–303. [PubMed: 11796142]

Fukata M, Kaibuchi K. Rho-family GTPases in cadherin-mediated cell-cell adhesion. Nat Rev Mol Cell Biol 2001;2:887–897. [PubMed: 11733768]

Fukuda J, Kameyama M, Yamaguchi K. Breakdown of cytoskeletal filaments selectively reduces Na and Ca spikes in cultured mammal neurones. Nature 1981;294:82–85. [PubMed: 7197327]

Gumbiner BM. Regulation of cadherin-mediated adhesion in morphogenesis. Nat Rev Mol Cell Biol 2005;6:622–634. [PubMed: 16025097]

Hamburger V, Hamilton HL. A series of normal satges in the development of the chick embryo. J Morphol 1951;88:49–93.

Hatta K, Nose A, Nagafuchi A, Takeichi M. Cloning and expression of cDNA encoding a neural calcium-dependent cell adhesion molecule: its identity in the cadherin gene family. J Cell Biol 1988;106:873–881. [PubMed: 2831236]

Iftinca M, Hamid J, Chen L, Varela D, Tadayonnejad R, Altier C, Turner RW, Zamponi GW. Regulation of T-type calcium channels by Rho-associated kinase. Nat Neurosci 2007;10:854–860. [PubMed: 17558400]

Johnson BD, Byerly L. A cytoskeletal mechanism for Ca2+ channel metabolic dependence and inactivation by intracellular Ca2+ Neuron 1993;10:797–804. [PubMed: 8098608]

Jungling K, Eulenburg V, Moore R, Kemler R, Lessmann V, Gottmann K. N-cadherin transsynaptically regulates short-term plasticity at glutamatergic synapses in embryonic stem cell-derived neurons. J Neurosci 2006;26:6968–6978. [PubMed: 16807326]

Lampugnani MG, Zanetti A, Breviario F, Balconi G, Orsenigo F, Corada M, Spagnuolo R, Betson M, Braga V, Dejana E. VE-cadherin regulates endothelial actin activating Rac and increasing membrane association of Tiam. Mol Biol Cell 2002;13:1175–1189. [PubMed: 11950930]

Miyake Y, Inoue N, Nishimura K, Kinoshita N, Hosoya H, Yonemura S. Actomyosin tension is required for correct recruitment of adherens junction components and zonula occludens formation. Exp Cell Res 2006;312:1637–1650. [PubMed: 16519885]

Nollet F, Kools P, van Roy F. Phylogenetic analysis of the cadherin superfamily allows identification of six major subfamilies besides several solitary members. J Mol Biol 2000;299:551–572. [PubMed: 10835267]

Noren NK, Arthur WT, Burridge K. Cadherin engagement inhibits RhoA via p190RhoGAP. J Biol Chem 2003;278:13615–13618. [PubMed: 12606561]

Noren NK, Niessen CM, Gumbiner BM, Burridge K. Cadherin engagement regulates Rho family GTPases. J Biol Chem 2001;276:33305–33308. [PubMed: 11457821]

Ohkubo T, Ozawa M. p120ctn binds to the membrane-proximal region of the E-cadherin cytoplasmic domain and is involved in modulation of adhesion activity. J Cell Biol 1999;274:21409–21415.

Ozawa M. p120-independent modulation of E-cadherin adhesion activity by the membrane-proximal region of the cytoplasmic domain. J Biol Chem 2003;278:46014–46020. [PubMed: 12952959]

Pattillo JM, Artim DE, Simples JE Jr. Meriney SD. Variations in onset of action potential broadening: effects on calcium current studied in chick ciliary ganglion neurones. J Physiol 1999;514(Pt 3):719–728. [PubMed: 9882744]

Piccoli G, Rutishauser U, Brusés JL. N-cadherin juxtamembrane domain modulates voltage-gated Ca2+ current via RhoA GTPase and Rho-associated kinase. J Neurosci 2004;24:10918–10923. [PubMed: 15574742]

Polo-Parada L, Plattner F, Bose C, Landmesser LT. NCAM 180 acting via a conserved C-terminal domain and MLCK is essential for effective transmission with repetitive stimulation. Neuron 2005;46:917–931. [PubMed: 15953420]

Rubio ME, Curcio C, Chauvet N, Brusés JL. Assembly of the N-cadherin complex during synapse formation involves uncoupling of p120-catenin and association with presenilin 1. Mol Cell Neurosci. 2005

Rueckschloss U, Isenberg G. Cytochalasin D reduces Ca2+ currents via cofilin-activated depolymerization of F-actin in guinea-pig cardiomyocytes. J Physiol 2001;537:363–370. [PubMed: 11731570]

Sahai E, Marshall CJ. ROCK and Dia have opposing effects on adherens junctions downstream of Rho. Nat Cell Biol 2002;4:408–415. [PubMed: 11992112]

Shapiro L, Fannon AM, Kwong PD, Thompson A, Lehmann MS, Grubel G, Legrand JF, Als-Nielsen J, Colman DR, Hendrickson WA. Structural basis of cell-cell adhesion by cadherins. Nature 1995;374:327–337. [PubMed: 7885471]

Shewan AM, Maddugoda M, Kraemer A, Stehbens SJ, Verma S, Kovacs EM, Yap AS. Myosin 2 is a key Rho kinase target necessary for the local concentration of E-cadherin at cell-cell contacts. Mol Biol Cell 2005;16:4531–4542. [PubMed: 16030252]

Stanley EF. Single calcium channels on a cholinergic presynaptic nerve terminal. Neuron 1991;7:585–591. [PubMed: 1657055]

Straight AF, Cheung A, Limouze J, Chen I, Westwood NJ, Sellers JR, Mitchison TJ. Dissecting temporal and spatial control of cytokinesis with a myosin II Inhibitor. Science 2003;299:1743–1747. [PubMed: 12637748]

Takasu MA, Dalva MB, Zigmond RE, Greenberg ME. Modulation of NMDA receptor-dependent calcium influx and gene expression through EphB receptors. Science 2002;295:491–495. [PubMed: 11799243]

Takeichi M. The cadherin superfamily in neuronal connections and interactions. Nat Rev Neurosci 2007;8:11–20. [PubMed: 17133224]

Takeichi M, Abe K. Synaptic contact dynamics controlled by cadherin and catenins. Trends Cell Biol 2005;15:216–221. [PubMed: 15817378]

Tamura K, Shan WS, Hendrickson WA, Colman DR, Shapiro L. Structure-function analysis of cell adhesion by neural (N-) cadherin. Neuron 1998;20:1153–1163. [PubMed: 9655503]

Tanaka H, Shan W, Phillips GR, Arndt K, Bozdagi O, Shapiro L, Huntley GW, Benson DL, Colman DR. Molecular modification of N-cadherin in response to synaptic activity. Neuron 2000;25:93–107. [PubMed: 10707975]

Thoreson MA, Anastasiadis PZ, Daniel JM, Ireton RC, Wheelock MJ, Johnson KR, Hummingbird DK, Reynolds AB. Selective uncoupling of p120(ctn) from E-cadherin disrupts strong adhesion. J Cell Biol 2000;148:189–202. [PubMed: 10629228]

Togashi H, Abe K, Mizoguchi A, Takaoka K, Chisaka O, Takeichi M. Cadherin regulates dendritic spine morphogenesis. Neuron 2002;35:77–89. [PubMed: 12123610]

Troyanovsky RB, Sokolov E, Troyanovsky SM. Adhesive and lateral E-cadherin dimers are mediated by the same interface. Mol Cell Biol 2003;23:7965–7972. [PubMed: 14585958]

Troyanovsky RB, Laur O, Troyanovsky SM. Stable and unstable cadherin dimers: mechanisms of formation and roles in cell adhesion. Mol Biol Cell 2007;18:4343–4352. [PubMed: 17761538]

Uchida N, Honjo Y, Johnson KR, Wheelock MJ, Takeichi M. The catenin/cadherin adhesion system is localized in synaptic junctions bordering transmitter release zones. J Cell Biol 1996;135:767–779. [PubMed: 8909549]

Vandekerckhove J, Deboben A, Nassal M, Wieland T. The phalloidin binding site of F-actin. Embo J 1985;4:2815–2818. [PubMed: 4065095]

Wheeler DB, Randall A, Tsien RW. Roles of N-type and Q-type Ca2+ channels in supporting hippocampal synaptic transmission. Science 1994;264:107–111. [PubMed: 7832825]

Wheelock MJ, Johnson KR. Cadherin-mediated cellular signaling. Curr Opin Cell Biol 2003;15:509–514. [PubMed: 14519384]

White MG, Crumling MA, Meriney SD. Developmental changes in calcium current pharmacology and somatostatin inhibition in chick parasympathetic neurons. J Neurosci 1997;17:6302–6313. [PubMed: 9236240]

Wildenberg GA, Dohn MR, Carnahan RH, Davis MA, Lobdell NA, Settleman J, Reynolds AB. p120-catenin and p190RhoGAP regulate cell-cell adhesion by coordinating antagonism between Rac and Rho. Cell 2006;127:1027–1039. [PubMed: 17129786]

Wilk-Blaszczak MA, Singer WD, Quill T, Miller B, Frost JA, Sternweis PC, Belardetti F. The monomeric G-proteins Rac1 and/or Cdc42 are required for the inhibition of voltage-dependent calcium current by bradykinin. J Neurosci 1997;17:4094–4100. [PubMed: 9151726]

Wu J, Mariner DJ, Thoreson MA, Reynolds AB. Production and characterization of monoclonal antibodies to the catenin p120ctn. Hybridoma 1998;17:175–183. [PubMed: 9627058]

Yamagata M, Herman JP, Sanes JR. Lamina-specific expression of adhesion molecules in developing chick optic tectum. Journal of Neuroscience 1995;15:4556–4571. [PubMed: 7790923]

Yap AS, Niessen CM, Gumbiner BM. The juxtamembrane region of the cadherin cytoplasmic tail supports lateral clustering, adhesive strengthening, and interaction with p120ctn. J Cell Biol 1998;141:779–789. [PubMed: 9566976]

Yap AS, Brieher WM, Pruschy M, Gumbiner BM. Lateral clustering of the adhesive ectodomain: a fundamental determinant of cadherin function. Curr Biol 1997;7:308–315. [PubMed: 9133345]

Zhang W, Benson DL. Stages of synapse development defined by dependence on F-actin. J Neurosci 2001;21:5169–5181. [PubMed: 11438592]

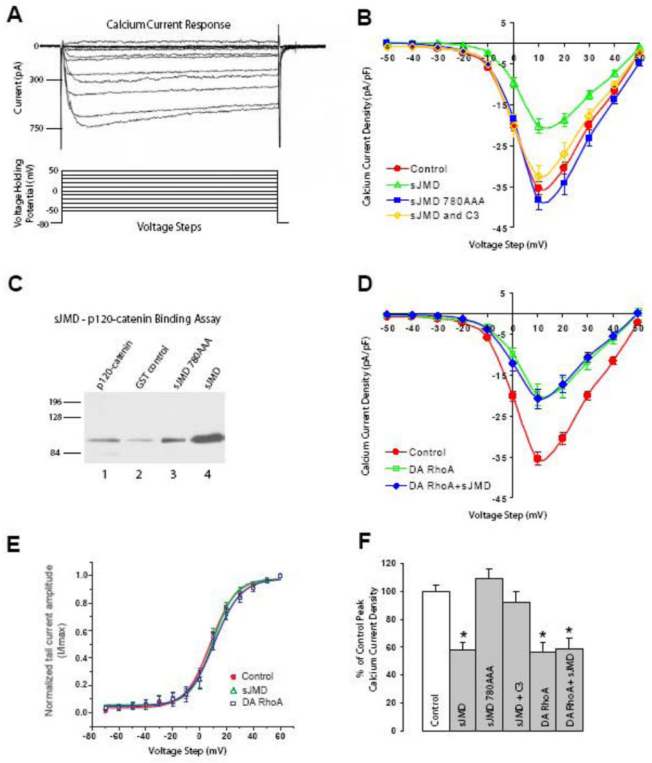

Figure 1. N-cadherin sJMD regulation of HVA Ca^{2+} current requires binding to p120-catenin and RhoA activation

A) Whole-cell voltage-clamp recordings of isolated inward Ca^{2+} currents from acutely dissociated ciliary ganglion neurons. Representative current response traces (*upper panel*) were elicited by 100 ms duration 10 mV steps in the voltage holding potential sequentially from −50mV to 50mV (*lower panel*). **B)** Current density plot shows averaged peak current reduction associated with infusion of N-cadherin sJMD as compared with control solution (control *circles* 35.4 ± 1.6, *n=21;* sJMD (1μM) *open triangles* 20.4 ± 1.8, *n=12*). Application of sJMD780AAA has no effect on current density (sJMD 780AAA (1μM) *squares* 38.4 ± 2.6, *n=8*). Simultaneous application of sJMD and C3 exotransferase substantially reverts peak current reduction associated with sJMD (sJMD (1μM) + C3 (0.5μM) *open diamonds* 32.5 ± 2.7, *n=6*). **C)** GST-tagged sJMD and GST-sJMD-780AAA were incubated with recombinant 6XHis-tagged p120-catenin (p120-228). Protein complexes were pulled down with glutathione-coated agarose beads, and analyzed by Western bolt with anti-His antibodies to detect p120-catenin. Lane 1, 5 μg of recombinant p120-228 runs at its predicted size of 89kDa. p120-catenin pulled down by recombinant GST (lane 2), sJMD-780AAA (lane 3), and sJMD (lane 4). Mutation of the p120-catenin binding site (sJMD-780AAA) substantially reduces p120-catenin binding to sJMD. **D)** Application of a dominant-active form of RhoA (DA-RhoA) reduces peak Ca^{2+} currents amplitude (DA-RhoA (0.4μM) *open squares* 19.8 ± 2.7, *n=8*). Simultaneous application of DA-RhoA and sJMD shows that their inhibitory effects are not additive (DA RhoA (0.4μM) + sJMD (1μM) *diamonds* 20.8 ± 2.5, *n=10*). **E)** Voltage dependence of activation obtained by plotting normalized tail current amplitude (I/Imax) against the voltage step. The continuous lines represent a Boltzmann fit of the data for control (*circles*), sJMD (*open triangles*), and DA RhoA (*open squares*). No difference in the activation profile was detected between treatments. Values are expressed as mean ± SE. **F)** Summary histogram showing averaged peak Ca^{2+} current density values for each condition tested in *C* and *E* expressed as a percentage of controls (100%). * Note significant decreases in HVA

Ca^{2+} current influx for sJMD ($p<0.001$), DA RhoA ($p<0.001$), and DA RhoA + sJMD ($p<0.001$) associated conditions.

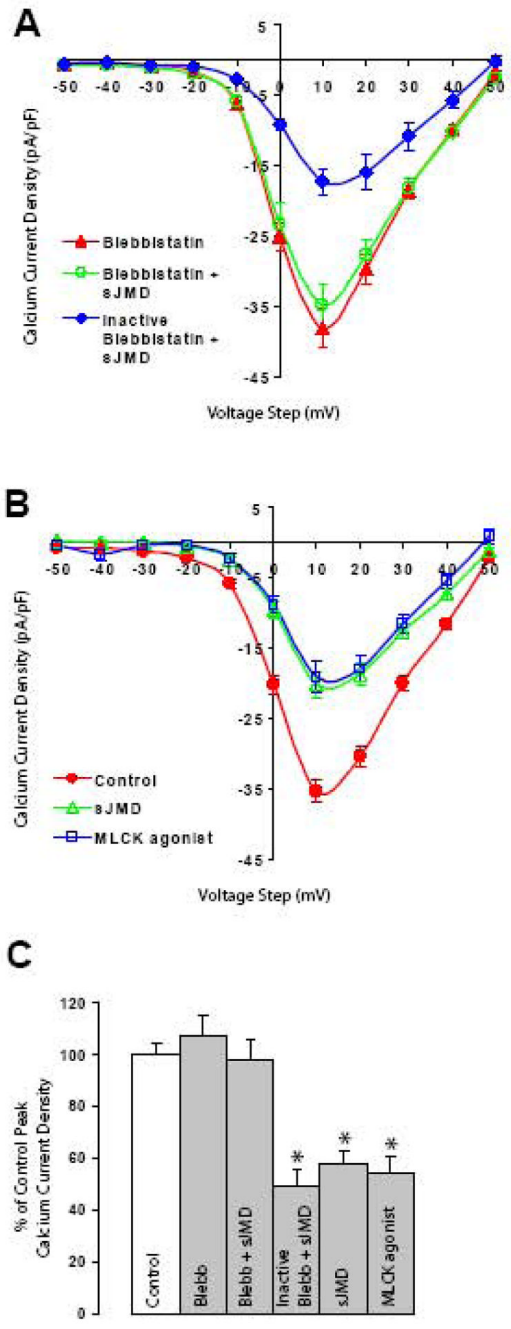

Figure 2. N-cadherin sJMD mediated Ca^{2+} current reduction requires actin-myosin interaction

A) Bath application of blebbistatin has no measurable effect on averaged peak Ca^{2+} currents (blebbistatin (50μM) *triangles* 38.1 ± 2.7, *n=11*). The presence of blebbistatin during pipette infusion of sJMD prevents current reduction (blebbistatin (50μM) + sJMD (1 μM) *open circles* 34.8 ± 3, *n=10*), indicating that sJMD signaling requires myosin interaction with actin. Photo-inactivated blebbistatin does not block sJMD reduction in Ca^{2+} current amplitude (inactive blebbistatin (50μM) + sJMD (1 μM) *diamonds* 17.3 ± 2, *n=6*). **B)** Infusion of an agonist peptide for myosin light chain kinase (MLCK) reduces averaged peak Ca^{2+} influx (control, *circles* 35.4 ± 1.6, *n=21;* sJMD (1μM) *open triangles* 20.4 ± 1.8, *n=12*; MLCK agonist (1μM) *open squares* 19.3 ± 2.1, *n=4*). Values are expressed as mean ± SE. **C)** Summary

histogram of results for averaged peak Ca^{2+} current density presented in *A* and *B* expressed as a percentage of control values (100%). Blebbistatin (*p=0.36*) and blebbistatin + sJMD (*p=0.85*) conditions are comparable to control, while inactivated blebbistatin + sJMD (*p<0.001*) and MLCK agonist (*p<0.001*) conditions show significant reduction. * *p<0.001*

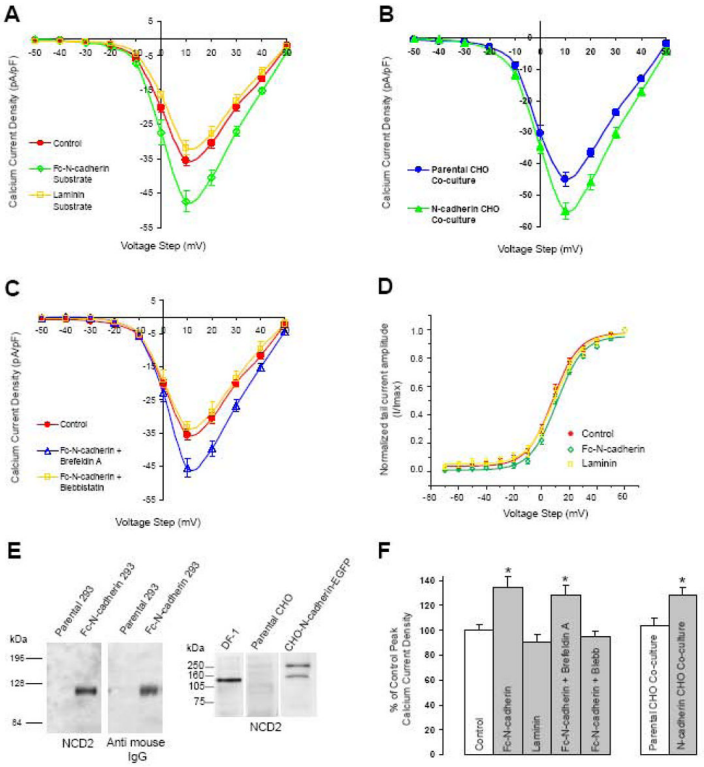

Figure 3. N-cadherin homophilic binding enhances HVA Ca^{2+} current amplitude

A) N-cadherin ectodomain C-terminally fused to an IgG Fc fragment (Fc-N-cadherin, 20μg/ml) was used as a substrate for plating dissociated St 40 ciliary neurons. Con A or laminin coated cover slips were used as controls. Ca^{2+} current density was analyzed 1-3h after plating (Con A, *circles* 35.4 ± 1.6, *n=21*; Fc-N-cadherin, *open diamonds* 47.7 ± 2.9, *n=13*; laminin, *open squares* 32 ± 2, *n=8*). **B)** Dissociated ciliary neurons were plated on CHO cells stably expressing full-length chicken N-cadherin C-terminally fused to EGFP and Ca^{2+} current amplitude was analyzed 6-8h after plating. Parental CHO cells devoid of N-cadherin expression (shown in E) were used as control (parental CHO, *circles* 45 ± 2.4, *n=12*; N-cadherin CHO, *triangles* 54.9 ± 2.6, *n=13*). **C)** Pre-incubation with brefeldin A (5mg/mL, 2hr) did not block Fc-N-cadherin induced peak Ca^{2+} current enhancement (control Con A, *circles* 35.4 ± 1.6, *n=21*; Fc-N-cadherin + brefeldin A, *open triangles* 45.5 ± 2.8, *n=8*). In contrast, bath application of blebbistatin blocked Fc-N-cadherin-mediated enhancement of averaged peak Ca^{2+} current (Fc-N-cadherin + blebbistatin (50μM) *open squares* 33.4 ± 1.8, *n=6*). **D)** Voltage dependence of activation obtained by plotting normalized tail current amplitude (I/Imax) against the voltage step. The continuous lines represent a Boltzmann fit of the data for control (*circles*), Fc-N-cadherin substrate (*diamonds*), and laminin (*squares*). **E)** Western blot analysis of recombinant Fc-N-cadherin used in **A** and CHO cell lines used for co-cultures in **B**. Left panel, HEK293 conditioned medium from parental and Fc-N-cadherin transfected cells immuno-blotted with anti-N-cadherin antibodies (*left*) or anti-mouse Fc fragment (*right*). Right panel, homogenates from parental or N-cadherin-EGFP transfected CHO cells immuno-blotted with anti-N-cadherin antibodies. Chicken fibroblast cell line (DF1 cells) homogenate was used as control (*lane 1*). Parental CHO cells are devoid of N-cadherin (*lane 2*). N-cadherin-EGFP runs at approximately 140kDa (*lane 3*), the additional band detected at ~240kDa may represent N-cadherin dimers. Values are expressed as mean ± SE. **F)** Summary histogram of the average peak Ca^{2+} current densities for the results presented in *A, B,* and *C* expressed as a percentage of their corresponding controls (100%). Left group, Fc-N-cadherin substrate vs control *

p<0.01; brefeldin A vs control * *p<0.01*. Right group, N-cadherin expressing CHO cells vs parental CHO cells * *p<0.05*.

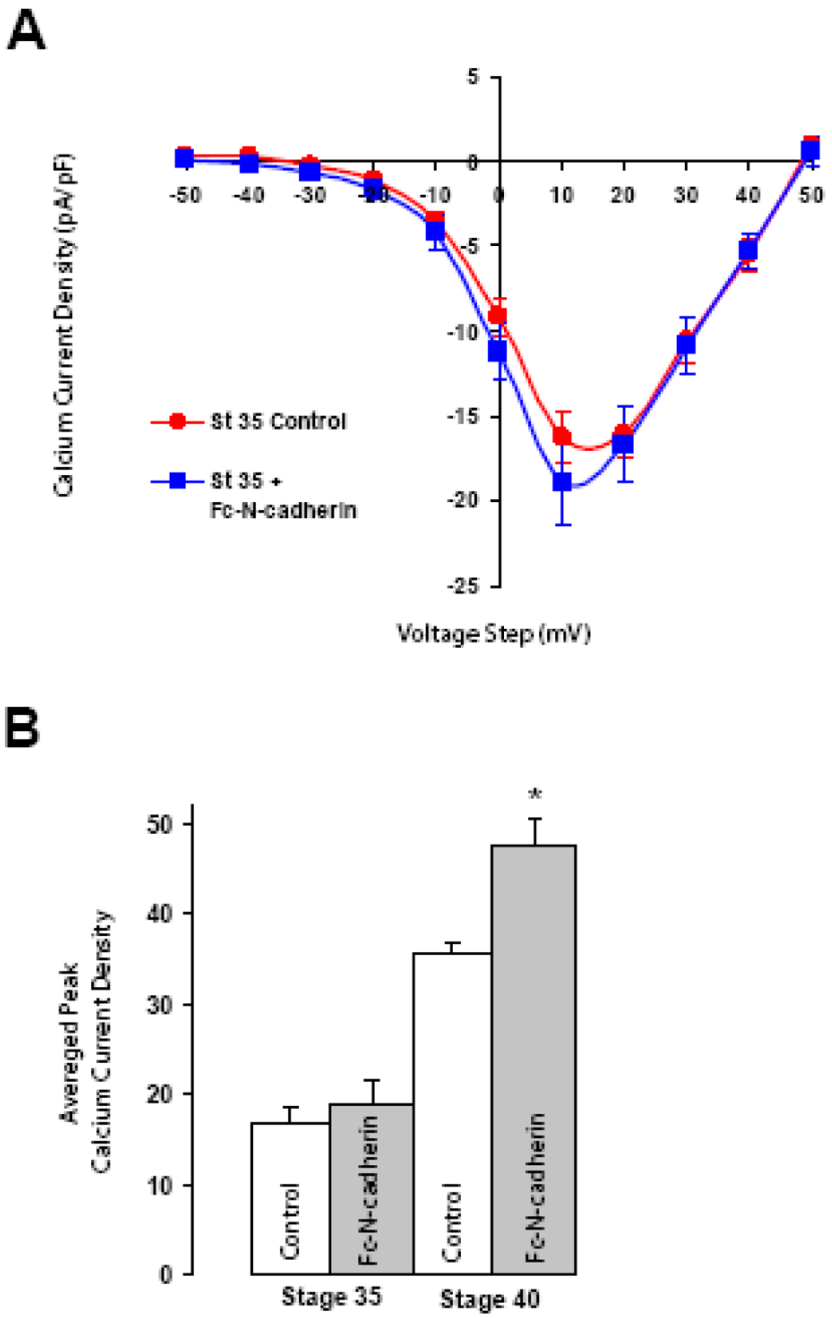

Figure 4. N-cadherin homophilic binding does not enhance HVA Ca^{2+} currents in St 35 neurons

A) Voltage clamp recordings from St 35 ciliary neurons plated on control Con A substrate or on Fc-N-cadherin substrate (Fc-N-cadherin). St 35 neurons show no substantial modulation of HVA Ca^{2+} current when plated on Fc-N-cadherin with respect to control (control *circles* 17 ± 1.5, *n=6*; Fc-N-cadherin substrate *squares* 18.9 ± 2.5, *n=7*, *p=0.27*). Values are expressed as mean ± SE. **B)** Summary histogram of the average peak Ca^{2+} current density recorded from St 35 and St 40 neurons plated on Con A or on an N-cadherin substrate (data from Fig 3A and 4A). * p<0.01

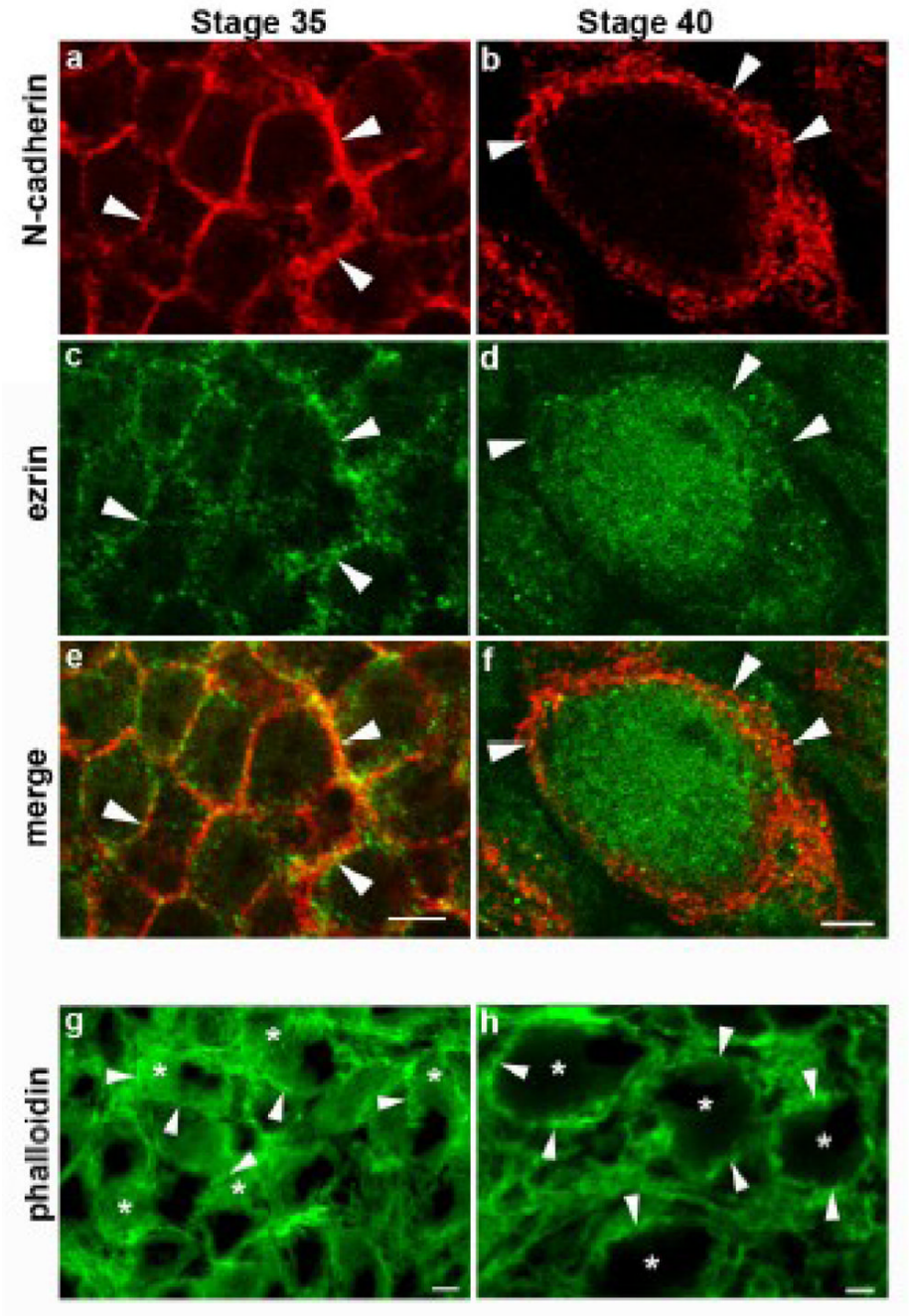

Figure 5. Development of ciliary neurons correlates with redistribution of ezrin and F-actin

Ciliary ganglia from St 35 and St 40 embryos were double stained with anti-N-cadherin (a, b) and antiezrin antibodies (c, d). Ezrin is localized to the membrane at St 35 and it becomes mostly cytosolic by St 40, suggesting a decrease in endogenous RhoA activity at St 40 as compared to St 35. g, h) Ciliary ganglion labeled with phalloidin-Alexa 488 to visualize the subcellular distribution of F-actin. Arrowheads in all panels point to the cell membrane. Scale bar in e for a, c, and e = 5μm; scale bar in f for b, d, and f = 5 μm, scale bar in g and h = 5 μm.

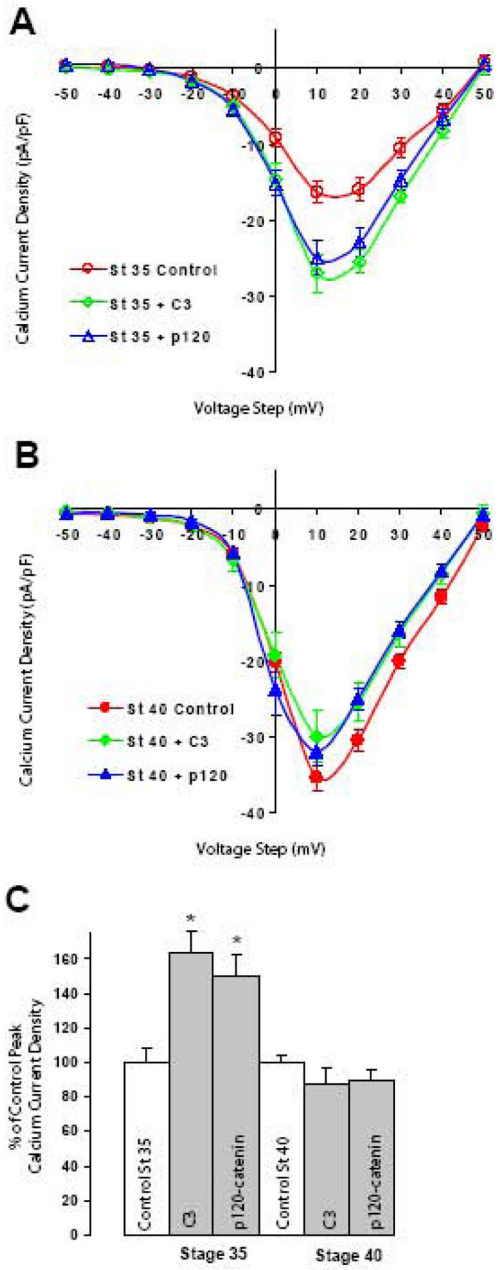

Figure 6. RhoA mediated inhibition of HVA Ca^{2+} currents is developmental regulated

A) Voltage clamp recording form St 35 ciliary neurons. Application of C3 exotransferase or p120-catenin (p120-228) protein results in enhancement (64% and 49% respectively) of averaged peak Ca^{2+} current amplitude as compared to control solution (control *open circles* 17 ± 1.5, *n=6*; C3 *open diamonds* 27.8 ± 2, *n=6*; p120-228 *open triangles* 25.4 ± 2.2, *n=7*). **B)** Application of C3 exotransferase or p120-catenin into St 40 ciliary neurons has no significant effect on peak Ca^{2+} current amplitude (control *circles* 35.4 ± 1.6, *n=21;* C3 (0.5μM) *diamonds* 31.1 ± 3.1, *n=10*; p120-288 (1μM) *triangles* 31.8 ± 1.9, *n=6*). Values are expressed as mean ± SE. **C)** Summary histograms of peak Ca^{2+} current densities for conditions reported in *A* and *B* expressed as a percentage of their respective controls (100%). At St 35 peak Ca^{2+} current density was significantly enhanced for both C3 (* *p<0.01*) and p120-catenin

(* $p<0.01$). In contrast, no significant effects were observed on St 40 neurons with both RhoA inhibitors (C3: 12% reduction, $p=0.16$; p120-catenin 10% reduction, $p=0.27$).

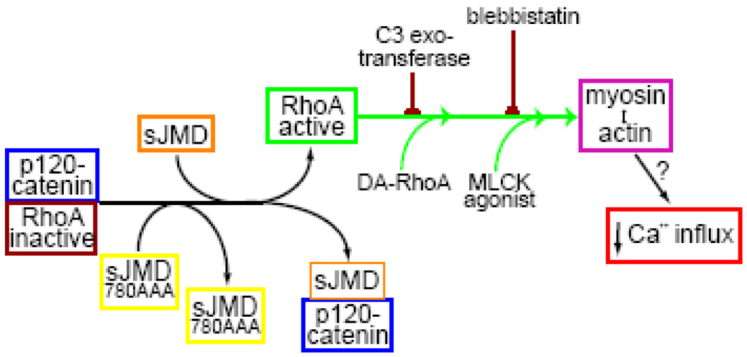

Figure 7. Diagram showing the element involved in the regulation of HVA Ca^{2+} influx downstream of RhoA activation by N-cadherin JMD

Infusion of sJMD into freshly dissociate St 40 ciliary neurons suppresses the inhibitory effect of p120-catenin on RhoA activity, presumably by disrupting a molecular complex required to inhibit RhoA. Application of a mutated sJMD (sJMD780AAA) which does not bind p120-catenin has no effect on Ca^{2+} influx. The activation of RhoA through this pathway negatively influences HVA Ca^{2+} influx by a mechanism that requires myosin interaction with actin. Co-application of sJMD with C3-exotransferase or blebbistatin suppresses the inhibitory effect of the sJMD on Ca^{2+} influx, indicating that the effect of sJMD is mediated by RhoA activation. In addition, both, DA-RhoA or an MLCK agonist, suppress Ca^{2+} influx similarly as infusion of sJMD.